

# Shear Induced Detachment of Microorganisms Attached to a Plane Wall

B. Boulbène\*, J. Morchain and P. Schmitz

Université de Toulouse; INSA, UPS, INP; LISBP, 135 Avenue de Rangueil, F-31077 Toulouse, France, INRA, UMR792 Ingénierie des Systèmes Biologiques et des Procédés, F-31400 Toulouse, France, CNRS, UMR5504, F-31400 Toulouse, France

\*Corresponding author: benjamin.boulbene@insa-toulouse.fr

**Abstract:** To reduce the risk of foodborne illnesses through the contamination of surfaces by bacteria, a better understanding of the cell-to-surface adhesion is required. Several approaches such as the study of the surface structure, morphology and physico-chemistry [1], the determination of the mechanical properties by AFM, or the analysis of microbial detachment in flow channels [2] already give some hints on the bacterial interaction with the surface.

We propose a numerical approach for the study of cell-to surface interaction under shear flow, which allowed to interpret experimental observations [3]. Such a study was already performed for blood or cancer cells [4]. Here the purpose is to calculate the force and torque exerted on a single cell submitted to a shear flow, in order to define the prevailing detachment mechanism, i.e., rolling or sliding motion. To this end, a three dimensional model of microorganism embedded at the bottom wall of a flow channel is developed using the COMSOL Multiphysics package. At this stage, we simulate the cell as a rigid obstacle, at first as a simple spherical object, then with more complicated shapes which geometry is similar to real bacteria shape. Force and torque are determined from the calculation of the flow around the obstacle using the steady state laminar Navier-Stokes model.

The spherical shape model matches analytical formulas accurately. For the spheroid and stick model, the influence of the flow orientation has also been investigated through a parametric solver. Though the deformability and inner structure of the cell are not yet taken into account, the present study is a first step to better understand cell behaviour observed in experimental assays.

**Keywords:** Cell adhesion – Shear stress

## 1. Introduction

Foodborne diseases represent an increasing health worldwide issue. From the

developing countries issues related to the food and water quality to the industrialized countries, with modern intensive agricultural practices, the risk exists, in the latter case, the bacteria getting even more resistant because of the use of antibiotics for instance. The global incidence of these diseases is difficult to evaluate. The European Food Safety Authority reported more than 5000 cases of foodborne outbreaks, causing about 45,000 human cases, 6,000 hospitalizations and 32 deaths in 2008 (EFSA Journal, 2008). More than the social consequences, it represents millions of Euros in terms of medical costs and loss of productivity for the economy.

In this work, we lay a foundation for the numerical study of bacteria adhered on food equipments under shear flow, in order to improve the removal methods. The three dimensional geometrical domain used represents the vicinity of a cell adhered to the channel flow bottom plate (fig.3). Previous studies [5] on the subject have treated the reorientation phenomenon without quantifying the stresses.

To compare our simulations to experimental assays, it is necessary to reproduce the same hydrodynamical conditions. The characterization of the experimental flow chambers led to the fact that adhered cells are within the laminar sublayer of the flow [2, 6]. Laminar Navier-Stokes application mode can therefore be employed to simulate the flow for our bacterial models. The resolution of the flow allows to integrate the stresses exerted on the cell model boundaries. The fluid domain is represented by a semi-sphere which dimension is about thirty times the size of the microorganism. The shape of the microorganism is removed from the domain. The walls created are thus considered as the walls of a rigid microorganism embedded on the bottom plate. An order of magnitude of the cell size is one micrometer.

## 2. Method

A set of models using different geometries was developed to analyze different cell shapes and variations amongst a population of cells having the same shape. The choice of using finite element analysis is too be able in a following step to take into account the cell structure and surface properties in order to simulate the deformations and adhesion.

The first case constitutes a validation case: stresses found through simulation on a sphere lying at the bottom plate of a flow channel by a shear flow is compared to the theory [7]. This shape can also represent microorganisms such as yeasts [2]. The calculation of the stresses based on geometry variation for a population are proportional to the mean shear stress  $\tau_w$  comprised within [1, 100 Pa] and to the square of the radius. No reorientation is foreseen since the object is kept spherical.

Then, a degree of complexity has been added. One of the axes in the horizontal plan has been lengthened. The degree of asymmetry implies the existence of a torque around the vertical and the flow axis when the cell is not facing the flow. According to experimental studies (not presented here), the first parameter is the ratio between the semi-axes length taken between 1 and 2, and the second parameter is the embedment of the cell from the almost full to the half cell in height to account for cell spreading [7].

Finally, the last case studied is a stick ( $2\mu\text{m}$  long and  $0.25\mu\text{m}$ , for the radius), to model bacillus bacteria. Another angular parameter has to be considered to account for a possible vertical position of the cell (fig 1).

Since parameterized geometry is not a feature available on COMSOL 3.5a, the cell shapes are created by hand. The parameters used in the solver are the horizontal angle and the average shear rate.

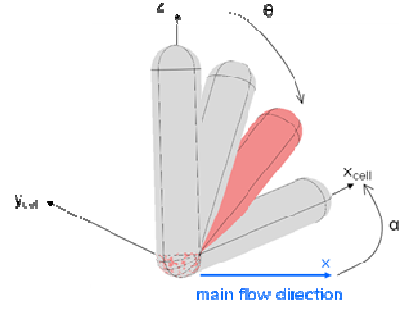


**Figure 1.** Angles regarding the flow direction for the stick case

## 3. Analytical Background

### 3.1 Reynolds number

According to the values found in the experimental assays, the particular Reynolds number is within the range  $[10^{-3}, 10^{-5}]$ .  $r_p$  is the radius of the sphere,  $\rho$  is the fluid density,  $\eta$  is the dynamic viscosity and  $\nu$  is the cinematic viscosity.

$$(1) \quad \eta = \rho\nu$$

$$(2) \quad \text{Re}_p = \frac{u(r_p)r_p}{\eta} = \frac{\rho r_p^2 \tau_w}{\eta^2}, \tau_w = \gamma\eta$$

### 3.2 Analytical stresses

For a sphere located at the bottom plate of a channel flow submitted to a shear flow, three stresses are to be taken into account : the drag, the torque along the transverse axis of the main flow [8] and the lift [9].

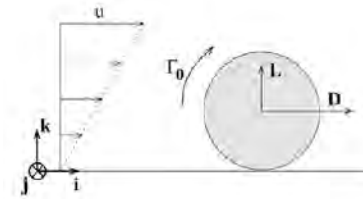


**Figure 2.** Shear induced stresses acting on a sphere at the bottom plate of channel flow

$$(3) \quad D = 32.0\tau_w r_p^2 + O(\text{Re}_p)$$

$$(4) \quad \Gamma_0 = 11.9\tau_w r_p^3 + O(\text{Re}_p)$$

$$(5) \quad L = 9.257 \tau_w r_p^2 \text{Re}_p$$

### 3.3 Domain reduction

As in the experiments the channel flow section is always far greater than the cell dimension, it was decided to reduce the domain studied to the vicinity of the cell. A spherical cell at the bottom plate of a shear does not disturb the shear flow beyond a 15 radius distance from the sphere [7]. Thus, a 30 radii semi-sphere was built as the domain, to ensure a sufficient condition, even for cells of more complex geometry.

### 4. Governing equations

In the vicinity of the cell, the flow is defined by the incompressible steady Navier-Stokes equations (eq. 6, 7).

$$(6) \quad \rho(\mathbf{u} \cdot \nabla) \mathbf{u} = \nabla[-p\mathbf{I} + (\nabla \mathbf{u} + (\nabla \mathbf{u})^T)] + \mathbf{F}$$

$$(7) \quad \nabla \cdot \mathbf{u} = 0$$

#### 4.1 Domain parameters

In these equations, the constants have been set to the water physical characteristics for NTP:

$$\rho = 10^3 \text{ kg} \cdot \text{m}^{-3}, \eta = 10^{-3} \text{ Pa} \cdot \text{s}$$

#### 4.2 Boundary conditions

Cell boundaries have been set to a no slip condition (8)

$$(8) \quad \mathbf{u} = \mathbf{0}$$

A reference pressure has been set at the bottom of the semi-sphere (eq. 9).

$$(9) \quad P_{ref} = 0 \text{ Pa}$$

Since the cell is in the laminar sublayer, a linear profile has been set for the inlet and outlet boundaries (eq. 10, 11, 12) with the parameters  $\alpha$ , angle between the main flow direction and the longest axis of the cell, and  $\gamma$ , shear rate coefficient.

$$(10) \quad u_x = \gamma z \cos(\alpha)$$

$$(11) \quad u_y = \gamma z \sin(\alpha)$$

$$(12) \quad u_z = 0$$

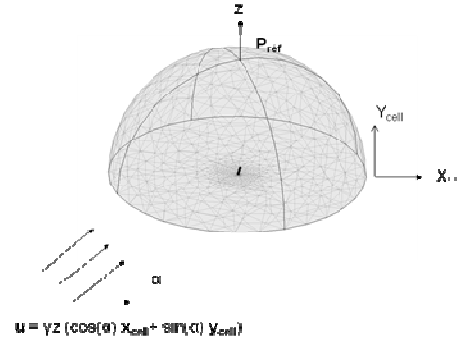


**Figure 3.** Mesh and external boundary conditions for the spheroid and stick case

### 5. Geometry/mesh

We had previously tried to solve the problem for a sphere with an almost punctual contact surface or for a complete one very close to the surface. But both cases could not be set because of the automatic meshing feature failure for the former, and for convergence of the calculations in the latter. It was then decided to embed the cell model. A contour is therefore common to the object walls and to the plate. The inner surface corresponding to this contour can be considered as an adhesion surface that we can modify if necessary. The volume of the sphere is kept at 98%.

The mesh is refined on the obstacle and broadens to the outer boundaries, since there are negligible variations in the external region.

#### 5.1 Solver parameters

A parametric solver using the BiCGStab method has been employed with the parameters  $\alpha$  (angle) and  $\gamma$  (shear rate). The triangular mesh size varies between 12000 elements for the sphere and 118000 for the stick.

## 5.2 Results output

Boundary integration variables were created to obtain the results in terms of drag, lift and torque.

For the validation case, the torque has been calculated at the center of the cell. For the other cases, we envisaged rotations around a point located on the boundary of the adhesion surface.

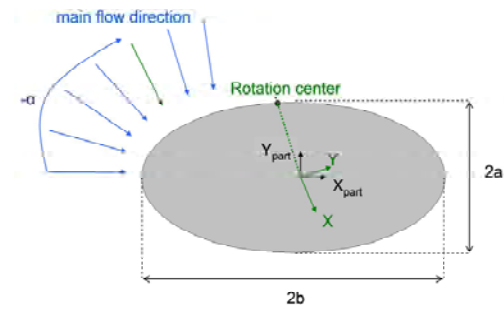


**Figure 4.** Geometrical parameters for the spheroid

## 6. Results

### 6.1 Validation case

The validation on the sphere case exhibits accurate results for the calculation of the drag and torque. The error is under 1.20% for the drag and under 3% for the torque. The error on the lift is close to 12% at its maximum. The variations as a function of the shear rate (fig.5) are plotted hereafter for a  $1\mu\text{m}$  radius sphere and fit the theory. It can be noticed that the drag and torque are more than one order of magnitude higher than the lift. Then we neglect the lift in the following parts. The choices in the geometry shape and size, and the boundary conditions are therefore validated.

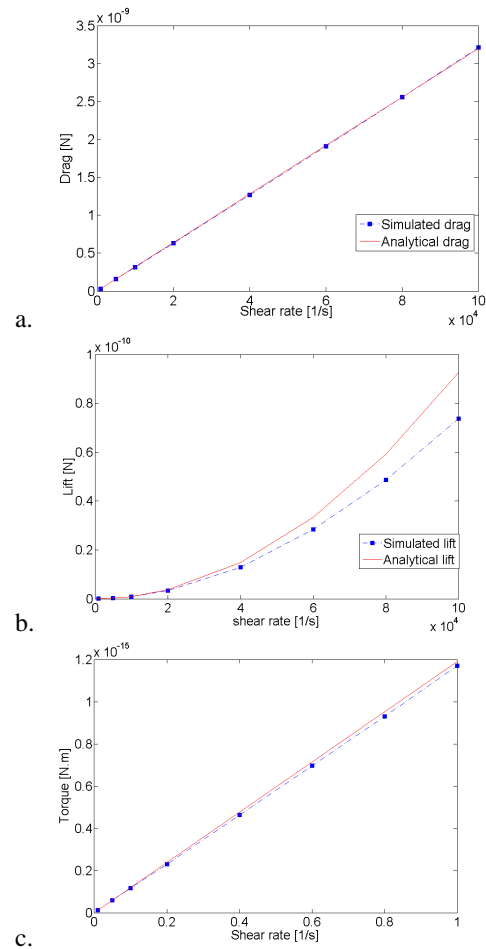


**Figure 5.** a. drag b. lift and c. torque acting on a sphere ( $r_p=1\mu\text{m}$ ) as a function of the shear rate  $\gamma$ . 2% of the sphere volume has been removed.

### 6.2 Spheroid case

Two geometrical parameters (length, embedment) and the orientation regarding the main flow ( $\alpha$ ) were investigated: the influence of the lengthening was studied for ( $\alpha=\frac{\pi}{4}$ ). For the length and angle related studies, the embedment height is  $0.1\mu\text{m}$ .

Two tendencies have been shown for the parameter length: on the one hand, the stress by surface unit is reduced when comparing to the sphere. The drag per surface unit is plotted on (fig.6.a). It decreased by 13% for  $b=2\mu\text{m}$ . The

reorientation component of the torque slightly increases as the length of the cell model (fig.6.a).

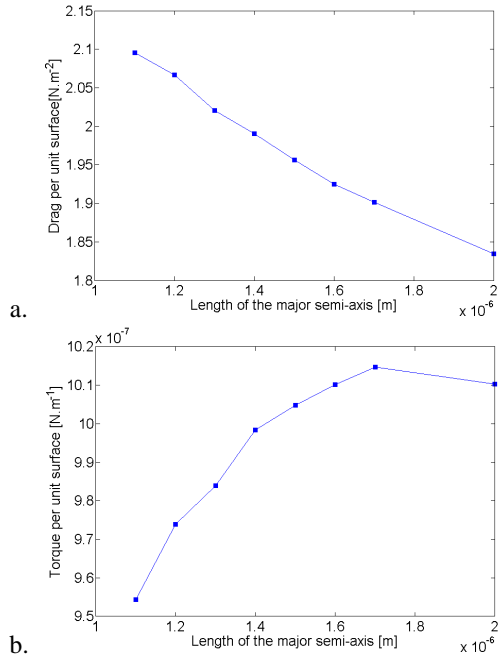


**Figure 6.** a. drag b. vertical component of the torque per unit surface for the spheroids ( $a = 10^{-6}$  m,  $b \in [1.1-2.0] \cdot 10^{-6}$  m,  $\alpha = \frac{\pi}{4}$ ,  $\gamma = 10^3 \text{ s}^{-1}$ )

When analyzing the problem through the orientation, the components of the torque along the vertical axis or the main flow axis cannot be neglected anymore. Three components have the same order of magnitude at their maximum: the transverse component maximum is two times greater than the others.

The embedment has been defined as the height of the cell removed from the bottom. This approaches a cell flattened on the plate or a cell placed in a protrusion. The drag is reduced by 4 four times when 90% of the lower half is removed. The rolling torque, i.e. the component along the transverse axis of the main flow, ratio is greater than 5.

### 6.3 Stick case

As for the stick case, several incidences regarding the vertical axis have been studied.

Cells with the smallest incidence experience a three times greater drag and a ten times greater rolling torque than cells lying on the surface.

The component of the torque along the main flow axis increases when the cell is lying. The torque along the vertical axis reaches its minimum for both extreme positions.

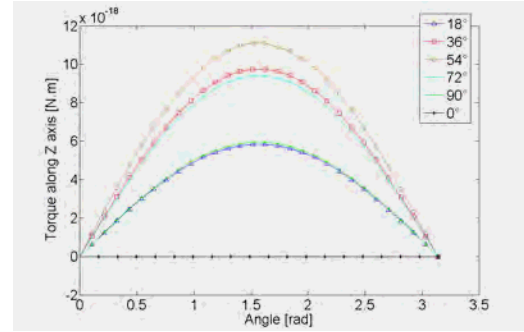


**Figure 7.** vertical component of the torque along the vertical direction for a stick ( $2 \cdot \mu\text{m} \cdot 0.25 \mu\text{m}$ ,  $\gamma = 10^3 \text{ s}^{-1}$ )

## 7. Conclusion

Calculation of the stresses exerted by shear flow on a single sphere shows good agreement with the theory. The use of a parametric solver for asymmetrical geometries is computationally cheap when carrying a study involving boundary conditions or abstract parameters. The investigation of several microorganisms shape behaviour with the variation of parameters such as the flow orientation and magnitude, or the geometry's size and orientation to the vertical axis gives a better understanding of the effect of heterogeneity in a cell population when it comes to detachment.

A further step would be to take into account cells' deformation. This step can be elucidated by the coupling of the Navier-Stokes, the structural mechanics and the deformed mesh application implemented in the fluid-structure interaction mode.

## 8. References

1. L.A. Olivier and G.A. Truskey A numerical analysis of forces exerted by laminar flow on spreading cells in a parallel plate flow chamber

- assay, *Biotechnology and Bioengineering* **42** 963 (1993).
2. M. Mercier-Bonin, K. Ouazzani, P. Schmitz, and S. Lorthois Study of bioadhesion on a flat plate with a yeast/glass model system, *Journal of Colloid and Interface Science* **271** 342 (2004).
  3. B. Boulbene, J. Morchain, and P. Schmitz Numerical 3D study of stresses exerted by a shear flow on various shaped adhered microorganism, submitted to *Appl. Environ. Microbiol.*, 2010
  4. P.W. Swapnil, D. Zhiqiang, M.B. Jordan, W.V. Mark, D. Tim, H.C. Kwan, and G. Lauren Cell Detachment Model for an Antibody-Based Microfluidic Cancer Screening System, *Biotechnology Progress* **22** 1426-1433 (2006).
  5. L. De La Fuente, E. Montanes, Y. Meng, Y. Li, T.J. Burr, H.C. Hoch, and M. Wu Assessing Adhesion Forces of Type I and Type IV Pili of *Xylella fastidiosa* Bacteria by Use of a Microfluidic Flow Chamber, *Appl. Environ. Microbiol.* **73** 2690-2696 (2007).
  6. S. Lorthois, P. Schmitz, and E. Anglés-Cano Experimental Study of Fibrin/Fibrin-Specific Molecular Interactions Using a Sphere/Plane Adhesion Model, *Journal of Colloid and Interface Science* **241** 52 (2001).
  7. S.B. Brooks and A. Tozeren Flow past an array of cells that are adherent to the bottom plate of a flow channel, *Computers & Fluids* **25** 741 (1996).
  8. M.E. O'Neill A sphere in contact with a plane wall in a slow linear shear flow, *Chemical Engineering Science* **23** 1293 (1968).
  9. G.P. Krishnan and J.D.T. Leighton Inertial lift on a moving sphere in contact with a plane wall in a shear flow, *Physics of Fluids* **7** 2538 (1995).

## 9. Acknowledgements

The authors gratefully acknowledge ANR INTERSPORE for its financial support..